

Measurement and Modeling of Electro-Chemical Properties of Ion Polymer Metal Composite by Complex Impedance Analysis

TARO NAKAMURA *, Tadashi IHARA *, Takashi HORIUCHI **,
Toshiharu MUKAI ***, and Kinji ASAKA ****

Abstract: The electrochemical and electromechanical characteristics of ion polymer metal composite (IPMC) are investigated using impedance analysis. The capacitance and resistance of IPMC are measured with various IPMC thicknesses, plating repetitions, and preheating times, which are the contributing factors of force generation. The generated force of IPMC increases with increasing IPMC thickness, number of plating repetitions, and extended preheating time. IPMC capacitance correlates with the generated force in all three cases, whereas IPMC resistance shows an independent change. These results show a strong correlation of the generated force of IPMC to its capacitance and structure and to the conditions for the IPMC fabrication process that increase its capacitance.

Key Words: soft material, ionic polymer, impedance analysis, actuator, medical device.

1. Introduction

Ion polymer metal composite (IPMC) is a newly developed “soft-actuator” material with many unique features [1]–[4], including extremely light weight, ease of control using low voltage, very fast response, and versatility in fabrication into various shapes and configurations. It is expected to be one of the most promising materials for artificial muscles and other medical devices. However, IPMC still has limited practical applications mainly owing to its relatively weak generated force. In this study, we study the electrochemical and mechanical characteristics of IPMC in order to identify the internal structure of IPMC that determines the magnitude of the generated force.

Preliminary studies [5]–[9] indicated that the generated force increases with increasing IPMC thickness, repeated plating, and preheating. The underlying mechanism of such an increase, however, remains to be clarified.

The goal of this study is to examine the changes in membrane resistance and membrane capacitance caused by these factors using impedance analysis with an equivalent circuit model.

2. Methods

2.1 IPMC Fabrication

IPMC was fabricated using a standard method [10] with original modifications. Nafion R-1100 resin was heat-pressed at 185°C at 3–12 MPa. IPMC thickness can be adjusted by changing the amount of resin, pressure, and time to heat press.

Table 1 shows the heat press time, the applied pressure, and

Table 1 Conditions for adjusting IPMC thickness.

Target Thickness [μm]	200	400	800
Nafion Resin [g]	3.0	6.2	9.0
Applied Pressure [MPa]	12	10	3
Heat Press Time [min]	7	4	9
Measured Thickness [μm] (mean \pm standard error)	241 \pm 2.4	481 \pm 9.8	1023 \pm 9.7

the amount of Nafion resin used for each target thickness of IPMC. Here, target thickness indicates the thickness of heat-pressed Nafion. When prepared as IPMC, the membrane swells as described below, and plating, immersion, and reduction increase the thickness. The actual membrane thicknesses in the final preparation of IPMC are listed under “measured thickness”. To simplify the description, the term “target thickness” is used in this article.

A flattened disk-shaped membrane was then immersed in the hydrolysis solution, which was a mixture of dimethyl sulfoxide (DMSO), potassium hydroxide (KOH), and water. The pre-processed membrane was immersed in $[\text{Au}(\text{phen})\text{Cl}_2]^+$ solution. After the immersion, the membrane was reduced with 5% Na_2SO_3 solution for gold plating. Plating or immersion and reduction was repeated 4 times to increase the thickness of the gold plate surface.

Figure 1 illustrates the IPMC inner structure observed by scanning electron microscopy (SEM). Between the gold plate formed and the inner Nafion layer, a region where gold intruded into the Nafion polymer is clearly seen. This intrusion area forms a complex dendrite-like structure, and the boundary between the gold metal and the Nafion polymer has a large surface area which forms an electric double-layer surface when electric field is applied.

IPMC membranes with thicknesses of 200 μm , 400 μm , and 800 μm (target thickness) were cut into 10 mm by 20 mm rect-

* Department of Clinical Engineering, Suzuka University of Medical Science, Suzuka 510-0293, Japan

** Division of Chemistry for Materials, Faculty of Engineering, Mie University, Tsu 514-8507, Japan

*** RIKEN-TRI Collaboration Center for Human-Interactive Robot Research, Nagoya 463-0003, Japan

**** National Institute of Advanced Industrial Science and Technology, Ikeda 563-8577, Japan

E-mail: ihara@suzuka-u.ac.jp

(Received May 12, 2009)

(Revised September 25, 2009)

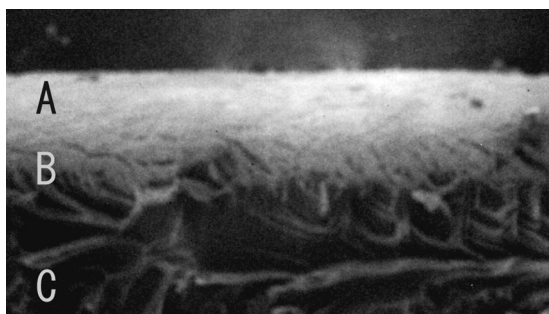


Fig. 1 SEM image of IPMC. A: Gold plate; B: Boundary area: gold electrode penetrating into Nafion layer; C: Nafion layer.

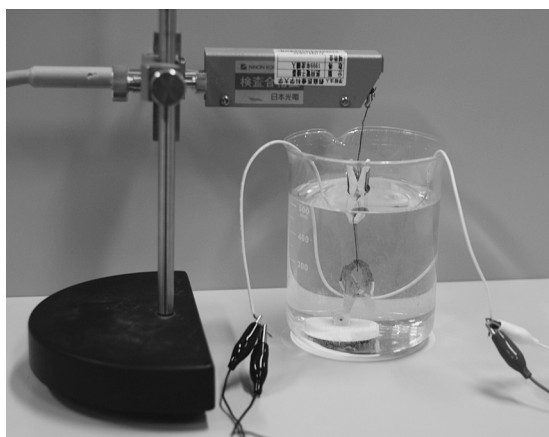


Fig. 2 Force measurement of IPMC by isometric transducer.

angular slices.

2.2 Measurement of Generated Force

Each of the 10 mm by 20 mm rectangular IPMC slices prepared was fixed on an electrode table in water. The IPMC slices were fixed with a clamp electrode such that the electrode held IPMC over 5 mm from the bottom. The other side of IPMC was held with another clamp electrode connected to an isometric transducer (Nihon Kodens Co., TB-651T, Fig. 2). IPMC was driven by a galvanostat unit (Hokuto Denko Co. HA151). An isometric transducer located just above the prepared IPMC measured generated force under the condition that no displacement occurs while exerting force. Since IPMC exhibits bending motion, the force measured in this setting is the component of IPMC generated force parallel to the IPMC surface (Fig. 3, F_m). Thus, the measured isometric force is the vertical component, which is parallel to the IPMC surface, of the generated force while IPMC is initiating bending motion but not inducing displacement. The applied current range is 0–300 mA. The main reason we measured isometric force is that it eliminates the effect of altered shape by bending and enables a more precise comparison of the generated force under the conditions we used.

2.3 Impedance Measurement

A precision LCR meter (Hewlett Packard 4284 A) was used to measure the impedance of the IPMC prepared. Impedance was measured over a range of 20–100 kHz in ascending order in air immediately after being taken out of water, in order to minimize the change in impedance as IPMC dries out. The applied current in the impedance measurement was 300 mA. We



Fig. 3 Illustration of IPMC bending motion and measured force: F_m (measured force element or force element parallel to IPMC) and F_p (force element perpendicular to IPMC).

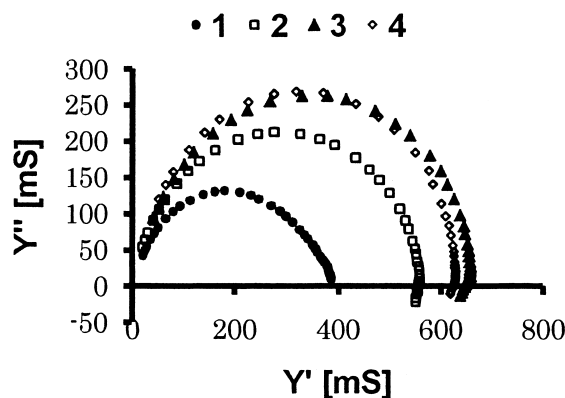


Fig. 4 Cole-Cole plot in admittance of plating repetition (1–4 times) experiment on IPMC.

used a simple resistor-capacitor (R-C) series model of IPMC and analyzed its resistance and capacitance using a Cole-Cole plot. Admittance rather than impedance was used to analyze a simple R-C series model because resistance can be obtained directly from the plot as the diameter of the half-circle of the Cole-Cole plot. Capacitance was calculated from the resistance obtained and the frequency at the peak of the half-circle of the Cole-Cole plot. Figure 4 shows the Cole-Cole plot in admittance for a plating repetition experiment. Impedance measurement was carried out under three different conditions: with variations in IPMC thickness, the number of plating repetitions, and preheating time.

3. Results

3.1 IPMC Characteristics vs. IPMC Thickness

The generated force measured by the isometric transducer, as well as membrane resistance and capacitance, is now summarized.

First, the generated force is demonstrated as a function of applied current for IPMCs of three different thicknesses (Fig. 5). The measured generated forces are shown as mean \pm standard error (SE) for three measurements at each point. It is demonstrated that the generated force increases almost linearly in the applied current range of 0–300 mA. The generated force also increases with IPMC thickness. The increase in the generated force, however, was not proportional to membrane thickness. The generated force of the 800 μm membrane was about 6.5-fold larger than that of the 200 μm IPMC. The generated force of the 400 μm IPMC was only about 2-fold that of 200 μm IPMC.

IPMC resistance, as measured by the impedance analysis re-

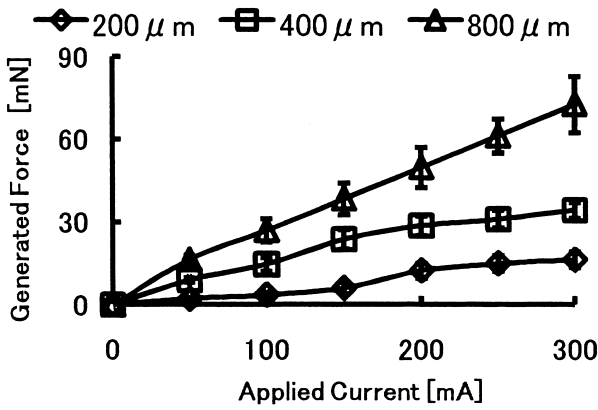


Fig. 5 Generated force of IPMCs of different thicknesses.

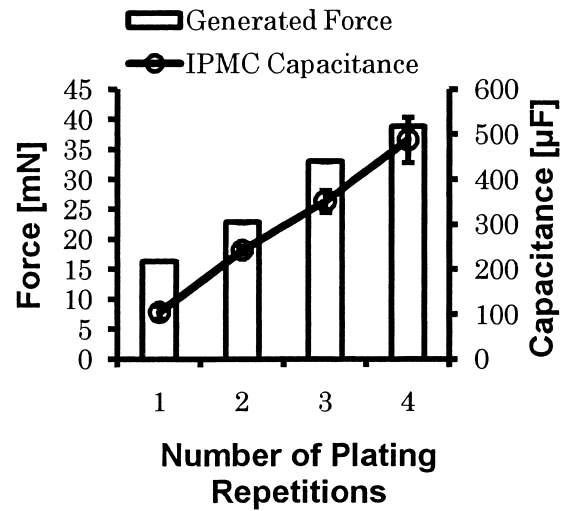


Fig. 8 IPMC capacitance vs. number of plating repetitions (mean±SE, n=3).

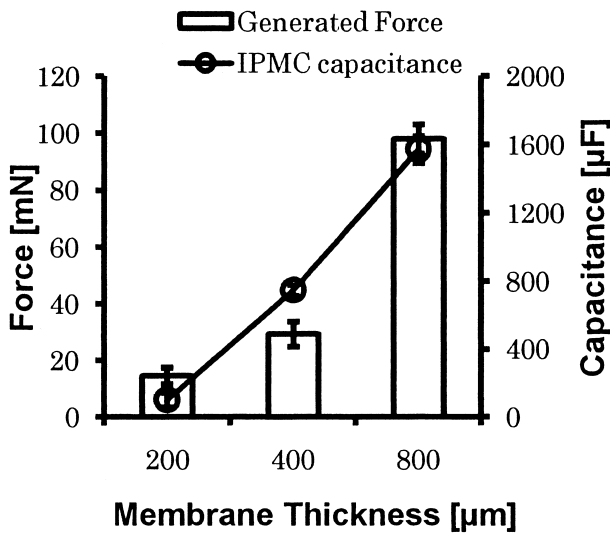


Fig. 6 IPMC capacitance vs. membrane thickness (mean±SE, n=3).

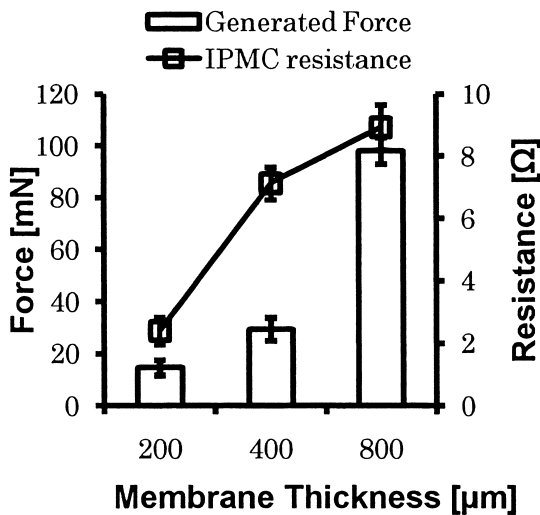


Fig. 7 IPMC resistance vs. membrane thickness (mean±SE, n=3).

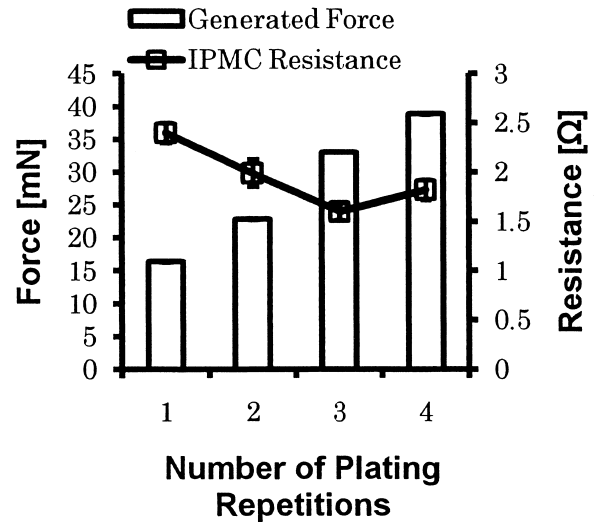


Fig. 9 IPMC resistance vs. the number of plating repetitions (mean±SE, n=3).

3.2 IPMC Characteristics vs. Number of Plating Repetitions

In this study, chemical plating was performed on Nafion 117 membranes. Only in this experiment was Nafion 117 used. Because the purpose of this experiment was to compare the effect of the number of plating repetitions, we eliminated the effect of variation in the process before the plating, including pre-heating, heat press, and hydrolysis. The rest of the IPMC fabrication process was the same as that with the Nafion R-1100 resin starting from immersion in $[Au(phen)Cl_2]^+$ solution as described above.

Figure 8 shows a plot of the generated force vs. the number of plating repetitions at an applied current of 300 mA. The larger the number of plating repetitions, the greater the generated force observed. With four platings, the generated force increased by approximately 2.5-fold that of a single plating.

As for membrane resistance, it decreased for up to three platings but slightly increased for four platings, which is comparable to that for two platings (Fig. 9).

On the other hand, membrane capacitance increased constantly with the number of plating repetitions up to 2.5-fold for

vealed increased capacitance with increased IPMC thickness (Fig. 6). Capacitance, however, showed no linear increase with IPMC thickness. The capacitance of the 400 μm IPMC was 3-fold that of the 200 μm IPMC, whereas that of the 800 μm IPMC was very large, namely, 9-fold that of the 200 μm IPMC. IPMC resistance also increased with increasing IPMC thickness (Fig. 7). The increase was almost linear to the thickness.

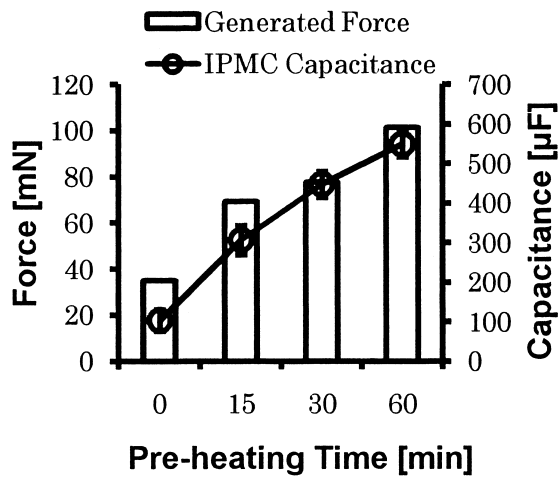


Fig. 10 IPMC capacitance vs. preheating time (mean±SE, $n=9$).

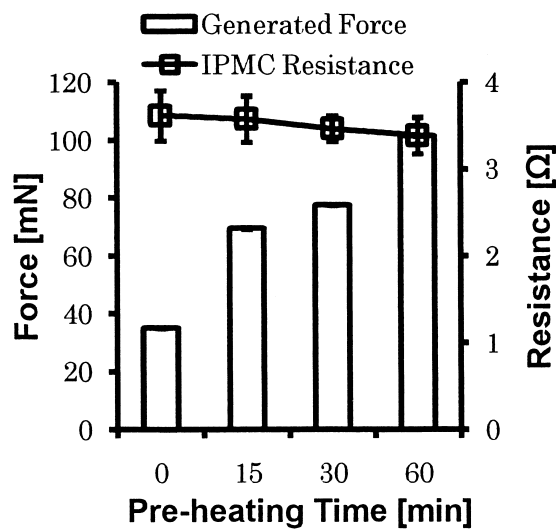


Fig. 11 IPMC resistance vs. preheating time (mean±SE, $n=9$).

four platings as compared with that for a single plating.

3.3 IPMC Characteristics vs. Preheating Time

The generated force increased with the preheating time before heat press. With a 60-min preheating time, the generated force of IPMC was 2.5-fold as high as that without preheating. This increase was parallel to the increase in membrane capacitance (Fig. 10). The capacitance of IPMC with a 60-min preheating was 5-fold that of IPMC without preheating.

Membrane resistance, on the other hand, showed no significant change with preheating time (Fig. 11).

4. Discussion

The aim of this study was to clarify the relationship between the force generation and structure of IPMC as well as the fabrication process. In addition, the underlying mechanism of the factors contributing to force generation was examined by impedance analysis.

4.1 IPMC Force Generation and Mechanism of IPMC Actuation

The fundamental mechanical features of IPMC actuation are currently being investigated [11]–[13]. Asaka et al. [14]–[16] have demonstrated that IPMC is driven by the applied current

rather than by the electric field developed. They also suggest a mechanism of IPMC operation, which is described as contraction at the cathode and expansion at the anode of IPMC. The principal mechanism is assumed to be the movement of counterions accompanied by trapped water molecules being driven by the current applied on both sides of IPMC. Our results of increased generated force in proportion to the applied current conform to this theory.

In this study, isometric force generation was measured rather than the conventional measurement with a load cell. This method measures the internal force of IPMC independently of the displacement associated with bending motion. It measures the internal contractile force in the longitudinal direction rather than the generated force tangential to the membrane surface. Moreover, it is a standard method in measuring isometric contraction in biological muscles and enables a more precise comparison of force generation under the conditions used in these experiments without being affected by the change in IPMC shape. The results showing that the generated force is related to IPMC capacitance is explained by the increase in Nafion-Gold plating boundary surface area, which can be described as a complex fractal-like structure (Fig. 1). The increased surface area is associated with the increased electrical double-layer surface area and increased capacitance. The increase in electrical double-layer area generates an increase in internal force developed by the electrical double layer, in that it exerts a greater force on the counterion inside IPMC.

4.2 IPMC Impedance Analysis

The principal electrochemical behavior of IPMC is well described with a simple lumped resistor-capacitor series circuit. The gold plating surfaces on both sides have a ramped resistor element, and the Nafion-gold plating boundary is represented by a capacitance element.

In our study, the increase in the generated force of IPMC with increased membrane thickness is considered to be related to the increased stiffness and increased electric double-layer surface area. Although the increased stiffness could simply be attributed to the increased dimensions, the increase in double-layer surface area may be for two reasons: (1) more counterions are contained in a thicker IPMC membrane, and (2) the deeper penetration of a gold electrode into a Nafion layer could result in a thicker boundary region, thereby increasing total electrode surface area as described above.

Repeated plating also increased membrane capacitance. This is again due to the increase in total electrode surface area made possible by the deeper penetration of the gold electrode into the Nafion layer. The generated force increases with an increase in the number of plating repetitions because the electric double-layer area, that is, the amount of charge at the electrode, increases. On the other hand, membrane resistance decreases as the conducting electrode layer thickens, which decreases the resistance along the longitudinal direction over the electrode surface. The deeper penetration of the electrode into the Nafion layer also shortens the effective interelectrode distance, which decreases the resistance across the Nafion layer. The resistance was slightly elevated when the plating was repeated four times. This may indicate the saturation of the above-described effect.

A longer preheating time also increased capacitance and generated force. The effect of preheating may be attributed to

the uniformization and crystallization of the Nafion structure as Nafion resin melts. The dielectric constant of heat-pressed Nafion decreases as micro-air bubbles are driven out, and the distance between the electrode surface and the center of each ion shortens.

Resistance, however, is not affected by preheating time presumably because it depends chiefly on the plating process after the heat press. The exact mechanism of the effect of preheating has yet to be examined.

4.3 Impedance Analysis with Constant Phase Element

The actual Cole-Cole plot of IPMC was not a true half-circle but rather a circle with a center shifted downward or a depressed circle indicating a constant phase element (CPE). The origin of this element is considered to be either the surface roughness of the electrode, the distribution of reaction rates, the variation in thickness or composition, or a nonuniform current distribution [17].

If the capacitance in the RC series circuit model is replaced with a CPE (Fig. 12), the admittance of the system can be described as

$$Z_{CPE} = \frac{1}{(j\omega)^p T}$$

where T denotes the CPE constant and p denotes the CPE index. The CPE index p varies between 0 and 1. When $p=1$, the impedance of CPE is identical to the capacitor impedance and T becomes equivalent to the capacitance. Thus, p indicates the deviation from the ideal capacitive impedance.

$$\begin{aligned} \frac{1}{Y} &= \frac{1}{R} + (j\omega)^p T \\ Y &= Y' - jY'' \\ &= \frac{R(1+AC)}{(1+AC)^2 + S^2A^2} - j \frac{RAS}{(1+AC)^2 + S^2A^2} \end{aligned}$$

Here,

$$\begin{aligned} A &= RT\omega^p, \\ C &= \cos\left(\frac{\pi}{2}p\right), \\ S &= \sin\left(\frac{\pi}{2}p\right). \end{aligned}$$

Table 2 shows the calculated parameters R , T , and p with the curve fit algorithm for experiment data of repeated plating.

The obtained values of $p = 0.77-0.86$ suggest a mildly contorted surface at the boundary. Resistance, as in the simple series RC model, decreased significantly with repeated plating. Reaction rate and current distribution, as well as the electrode thickness at the Nafion-electrode boundary, may also vary because of the fractal structure. These remain to be examined in further studies.

Takagi et al. [18] developed a distributed constant model of IPMC and examined the effect of counterion on IPMC impedance. They found a larger resistance and a smaller capacitive element in IPMC with TEA (tetraethyl ammonium) as the counterion than in that with sodium ion as the counterion. Thus, the size of the counterion is another factor affecting IPMC impedance.

Further analysis of the IPMC actuation mechanism will help put IPMC into practical use.

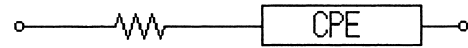


Fig. 12 Equivalent circuit model of IPMC with CPE.

Table 2 Calculated parameters of the equivalent circuit model of IPMC with CPE.

Repetition	R (Ω)	T	p
1	2.6	3.00E-06	0.77
2	1.7	1.20E-05	0.81
3	1.5	1.20E-05	0.85
4	1.5	1.20E-05	0.86

5. Conclusion

Our study indicates the following: (1) the generated force of IPMC is proportional to membrane thickness, the number of plating repetitions, and preheating time; (2) the increase in the generated force of IPMC is related to the increased membrane capacitance; (3) the membrane resistance of IPMC changes independently of membrane capacitance; (4) IPMC membrane characteristics may be described fairly well by a simple RC equivalent circuit model; (5) the capacitance of IPMC is the predominant factor in determining the generated force of IPMC; and (6) a measured Cole-Cole plot may be described better with a constant phase element model.

Acknowledgements

This work was supported in part by the Grants-in-Aid for Scientific Research (Nos. 17040024, 16500305, and 70261039) from the Ministry of Education, Culture, Sports, Science and Technology, Japan and by a grant (AOARD-03-4037) from the Asian Office of Aerospace Research and Development.

References

- [1] T. Ihara, Y. Ikada, T. Nakamura, T. Mukai, and K. Asaka: Solid polymer electrolyte membrane flow sensor for tracheal tube, *SPIE's 13th Annual International Symposium on Smart Structures and Materials*, pp. 61670U-1-61670U-8, 2006.
- [2] K.J. Kim and M. Shahinpoor: A novel method of manufacturing three-dimensional ionic polymer-metal composites (IPMCs) biomimetic sensors, and artificial muscles, *Polymer*, Vol. 43, No. 3, pp.797-802, 2002.
- [3] M. Yamakita, N. Kamamichi, Y. Kaneda, K. Asaka, and Z.W. Luo: Development of an artificial muscle linear actuator using ionic polymer-metal composites, *Advanced Robotics*, Vol. 18, No. 4, pp. 383-399, 2004.
- [4] S. Guo, Y. Okuda, W. Zhang, X. Ye, and K. Asaka: The development of a hybrid type of underwater micro biped robot, *Journal of Applied Bionics and Biomechanics*, Vol. 3, No. 3, pp. 143-150, 2006.
- [5] T. Ihara, T. Nakamura, Y. Ikada, K. Oguro, and K. Asaka: Fabrication of solid polymer electrolyte membrane for medical use and its mechanical characteristics under biomimetic circumstances, *Proceedings of the 6th Asian-Pacific Conference on Medical and Biological Engineering*, (CD-ROM), PA-2-79, 2005.
- [6] T. Nakamura, T. Ihara, S. Umeda, Y. Ikada, K. Oguro, and K. Asaka: A new biomedical sensor using solid polymer electrolyte membrane, *Proceedings of the 6th Asian-Pacific Conference on Medical and Biological Engineering*, PA-2-78, 2005.
- [7] T. Ihara, T. Nakamura, Y. Ikada, K. Asaka, K. Oguro, and N. Fujiwara: Application of a solid polymer electrolyte

membrane-gold to an active graft, *Proceedings of the 2nd International Conference on Artificial Muscle*, Session IV-2, 2004.

- [8] T. Ihara, T. Nakamura, T. Nakamura, Y. Ikada, K. Asaka, N. Fujiwara, and K. Oguro: Isotonic tension and isometric displacement measurement of a solid polymer electrolyte membrane-gold, *Proceedings of the first International Congress on Biomimetics and Artificial Muscle*, T4-1, 2002.
- [9] T. Ihara, T. Masuda, T. Nakamura, Y. Ikada, K. Asaka, N. Fujiwara, and K. Oguro: Isotonic tension and isometric displacement measurement of a solid polymer electrolyte membrane-gold, *Proceedings of the Society of Instrument and Control Engineers*, TA1-17-3 (0745), 2003.
- [10] N. Fujiwara, K. Asaka, Y. Nishimura, K. Oguro, and E. Torikai: Preparation of gold-solid polymer electrolyte composites as electric stimuli-responsive materials, *Chemistry of Material*, Vol. 12, No. 6, pp. 1750–1754, 2000.
- [11] P.G. de Gennes, K. Okumura, M. Shahinpoor, and K.J. Kim: Mechanoelectric effects in ionic gels, *Europhysics Letters*, Vol. 50, pp. 513–518, 2000.
- [12] K.M. Newbury and D.J. Leo: Linear electromechanical model of ionic polymer transducers – Part I: Model development, *Journal of Intelligent Material Systems and Structures*, Vol. 14, pp. 333–342, 2003.
- [13] K.M. Newbury and D.J. Leo: Linear electromechanical model of ionic polymer transducers – Part II: Experimental validation, *Journal of Intelligent Material Systems and Structures*, Vol. 14, No. 6, pp. 343–357, 2003.
- [14] K. Asaka, K. Oguro, Y. Nishimura, M. Mizuhata, and H. Takenaka: Bending of polyelectrolyte membrane-platinum composites by electric stimuli I. Response characteristics to various waveforms, *Polymer Journal*, Vol. 27, No. 4, pp. 436–440, 1995.
- [15] K. Asaka and K. Oguro: Bending of polyelectrolyte membrane-platinum composites by electric stimuli Part II. Response characteristics to various waveforms, *Journal of Electroanalytical Chemistry*, Vol. 480, No. 1-2, pp. 186–198, 2000.
- [16] K. Asaka and K. Oguro: Bending of polyelectrolyte membrane-platinum composites by electric stimuli III: Self-oscillation, *Electrochim. Acta*, Vol 45, No. 27, pp. 4517–4523, 2000.
- [17] J-B Jorcin, M.E. Orazem, N. Pebere, B. Tribollet: CPE analysis by local impedance analysis, *Electrochim. Acta*, Vol. 51, No. 8-9, pp. 1473–1479, 2006.
- [18] K. Takagi, Y. Nakabo, Z-W. Luo, and K. Asaka: On counterion doping effect to electrical impedance change of IPMC actuator, *Proceedings of the 7th SICE System Integration Division Annual Conference*, pp. 177–178, 2006.

Taro NAKAMURA (Member)



He received his B.S. and M.S. degrees from the Suzuka University of Medical Science, Japan, in 2001 and 2003, respectively. In 2003, he joined the Department of Clinical Engineering of the Suzuka University of Medical Science, where he is currently a Research Assistant. His research interests include medical device systems.

Tadashi IHARA (Member)



He received his B.S. and M.S. degrees in health science from the University of Tokyo, Japan, in 1980 and 1982, respectively. He received his Ph.D. degree in Biomedical Engineering from Duke University in 1990. In 1993, he joined the faculty of the Suzuka University of Medical Science, where he is currently a Professor and Chairman of the Department of Clinical Engineering. His research interests include medical device systems and actuators. He is a member of IEEE, and SPIE.

Takashi HORIUCHI



He received his B.S. and M.S. degrees in chemical engineering from the Tokyo University of Science in 1976 and 1978, respectively. He received his Ph.D. degree in engineering from the University of Tokyo in 1987. In 2003, he joined the faculty of Mie University, where he is currently a Professor of the Department of Engineering. His research interests include biomaterials and artificial organs. He is a member of ASAIO, IFAO, and JSMBE.

Toshiharu MUKAI (Member)



He received his B.E., M.E. and D.E. degrees in mathematical engineering and information physics from the University of Tokyo in 1990, 1992 and 1995, respectively. He was a frontier research scientist in RIKEN, from April 1995 to September 2000. From October 2000 to September 2001, he stayed at Laboratoire de Neurobiologie in Marseille, France, as a postdoctoral fellow. He has been a laboratory head in RIKEN from October 2001. His current research interests include robot sensors, sensor fusion, active sensing, and artificial muscle. He is a member of IEEE, RSJ, and IEICE.

Kinji ASAKA (Member)



He received his PhD degree in science from Kyoto University in 1990. He is currently a Group Leader of the Artificial Cell Research Group, Research Institute for Cell Engineering of National Institute of Advanced Industrial Science and Technology (AIST). His current research interests include interfacial electrochemistry and polymer actuators. He is a member of SPSJ, RSJ and JSME.

.....